medRxiv preprint doi: https://doi.org/10.1101/2020.08.11.20172833; this version posted August 14, 2020. The copyright holder for this preprint (which was not certified by peer review) is the author/funder, who has granted medRxiv a license to display the preprint in perpetuity. All rights reserved. No reuse allowed without permission.

Lockdown Measures and their Impact on Single- and Two-age-structured Epidemic Model for the COVID-19 Outbreak in Mexico

J. Cuevas-Maraver
Grupo de Física No Lineal, Departamento de Física Aplicada I,
Universidad de Sevilla. Escuela Politécnica Superior, C/ Virgen de África, 7, 41011-Sevilla, Spain
Instituto de Matemáticas de la Universidad de Sevilla (IMUS). Edificio Celestino Mutis. Avda. Reina Mercedes s/n, 41012-Sevilla, Spain

P. G. Kevrekidis, Q. Y. Chen, and G. A. Kevrekidis
Department of Mathematics and Statistics, University of Massachusetts, Amherst, MA 01003-4515, USA

Víctor Villalobos-Daniel
National Center of Disease Prevention and Control Programs - CENAPRECE,
Avenida Benjamín Franklin, 132, 11800-Ciudad de México, CDMX

Z. Rapti
Department of Mathematics and Carl R.Woese Institute for Genomic Biology, University of Illinois at Urbana-Champaign

Y. Drossinos
European Commission, Joint Research Centre, I-21027 Ispra (VA), Italy

The role of lockdown measures in mitigating COVID-19 in Mexico is investigated using a comprehensive nonlinear ODE model. The model includes both asymptomatic and presymptomatic populations with the latter leading to sickness (with recovery, hospitalization and death possibilities). We consider the situation involving the imposed application of partial social distancing measures in the time series of interest and find optimal parametric fits to the time series of deaths (only), as well as to that of deaths and cumulative infections. We discuss the merits and disadvantages of each approach, we interpret the parameters of the model and assess the realistic nature of the parameters resulting from the optimization procedure. Importantly, we explore a model involving two sub-populations (younger and older than a specific age), to more accurately reflect the observed impact as concerns symptoms and behavior in different age groups. For definitiveness and to separate people that are (typically) in the active workforce, our partition of population is with respect to members younger vs. older than the age of 65. The basic reproductive number of the model is computed for both the single- and the two-population variant. Finally, we consider what would be the impact on the number of deaths and cumulative infections upon imposition of partial lockdown (involving only the older population) and full lockdown (involving the entire population).

NOTE: This preprint reports new research that has not been certified by peer review and should not be used to guide clinical practice.

medRxiv preprint doi: https://doi.org/10.1101/2020.08.11.20172833; this version posted August 14, 2020. The copyright holder for this preprint (which was not certified by peer review) is the author/funder, who has granted medRxiv a license to display the preprint in perpetuity. All rights reserved. No reuse allowed without permission.

I. INTRODUCTION

COVID-19, the disease caused by the novel coronavirus SARS-CoV-2 has, as of August 2020, affected 216 countries and changed the daily lives of billions of people [1]. It has at the same time been the focus of numerous studies, both clinical and mathematical in nature. The study of compartmental models that address the spreading of such epidemics has a time-honored history since the seminal contribution of [2], which by now has been summarized in various reviews [3] and books [4–6]. In recent years, variations to such models focusing on the particularities of coronaviruses have been incorporated, such as the role of asymptomatic carriers of the virus, both as regards earlier CoV examples, such as MERS (see for a related example the work of [7]), and lately in the case of COVID-19 (see for a related example the work of [8]).

Following on some of these more recent developments, the present study focuses on a comprehensive compartmental epidemiological model that takes into account some of the intricacies of COVID-19, while considering its applicability to an urgent and important case example, namely the country of Mexico. More specifically, the model is an extension of the standard SEIR (Susceptible, Exposed, Infectious, Recovered) model that includes a presymptomatic stage, during which a person experiences no symptoms, but is nevertheless infectious [9]. The proposed mathematical setup also accounts for both the asymptomatic infectious and symptomatic infectious individuals. Asymptomatic infectious cases have been found in numerous studies and reports argue that they may be significantly under-reported [8, 10], which may complicate mitigation efforts such as contact tracing and self-isolation. Those with severe disease symptoms may require lengthy hospitalization, which has strained the health system of many countries [11]. In light of that, the model also includes a compartment describing the hospitalizations. Another distinctive feature of the disease is the nonhomogeneity with which it manifests in different age groups, especially as it pertains to symptom severity and mortality risk [12, 13]. Other factors, such as preexisting conditions and intergenerational contacts may also play a role [14]. While population age-structure may be often averaged out and deemphasized in numerous modeling attempts [15], in our model we choose to consider both a single age-group and a two age-group version of the model. The rationale behind this choice is the multifold inhomogeneity in the population of various countries (including our example of interest). Firstly, as mentioned above, the severity in younger people (especially children [16]) is smaller than that in adults. Secondly, older and more vulnerable people may shed more viral particles, thus being more infectious [17]. Thirdly, contacts per day [18] and the contact network itself of older people is different from those of younger people. The partition especially between professionally active (i.e., non-retired) individuals and retirees is important in connection to the above two points, both as regards the differential in average number of contacts of these two groups, and as regards the potential vulnerabilities thereof.

As a case study, we focus on the COVID-19 outbreak in Mexico. While studies for Mexico based on mathematical models exist, they differ from ours in several significant ways. Some ignore social-distancing and other mitigation measures [19], others focus on the estimation of R_0 and infections, using a Bayesian hierarchical model [20], and yet others have since become outdated [21]. Mexico faces a unique challenge, due to the prevalence of COVID-19 risk factors, such as obesity, diabetes and hypertension, among its population [22]. This is being reflected in the reported data and our predictive results, which show almost as many fatalities in the < 65 years old group as in the > 65 years old group. We feel that these particular features of the Mexican population in conjunction with the large number of infections and especially of deaths in the country warrant an examination through the prism of different age-structured models (e.g., single-age vs. two-age models; in future studies, possibly further partitioning may be of interest) and an assessment of the potential impact of lockdown measures in the immediate future.

Following the formulation of the single-population model and the results obtained through it in section II, we continue with the two age-group model in section III. In each case, we obtain the optimal parameters of the model in matching the available data regarding deaths, which are considered to be the single most reliable piece of available information. We do discuss the advantages and disadvantages of potentially matching the number of cumulative infections (and the number of deaths). Once the optimal fitting parameters are obtained we assess the impact in both deaths (but also cumulative infections) of immediate lockdown measures in either the case of the entire population or in that of just the older age group. The prediction of the model is that thousands of lives may be saved in just the following month alone, should such measures be imposed effective immediately. In section IV we summarize our conclusions and present ideas for future investigation.

II. SINGLE-POPULATION MODEL

A. Equations

In the model presented herein, we modify somewhat the setup of the earlier work of a subset of the present authors [23], by incorporating the effect of presymptomatic individuals. More concretely, we start with a susceptible (S) population that can become exposed (E) to the SARS-CoV-2 virus upon interaction with three categories of already infected individuals: (a) the presymptomatic (P), individuals who are infected, infectious, and eventually will develop symptoms; (b) the asymptomatic (A), individuals who are infected, infectious, and will not develop (clinical) symptoms; and (c) the symptomatically infected/sick (I) population members carrying the virus (infectious). Upon such interaction, the susceptible become exposed to the virus.

medRxiv preprint doi: https://doi.org/10.1101/2020.08.11.20172833; this version posted August 14, 2020. The copyright holder for this preprint (which was not certified by peer review) is the author/funder, who has granted medRxiv a license to display the preprint in perpetuity. All rights reserved. No reuse allowed without permission.

Notice that in the susceptible population, there is the potential for "removal" (i.e., death) by other causes, via the last term of the corresponding ODE proportional to μ, however this term is practically irrelevant for our purposes. For this reason, we set $\mu = 0$.

Once a member of the population becomes exposed (E), a latent period ($\tau_l = 1/\sigma_1$) of the virus follows (expected to be in the vicinity of 3 days [24]), during which the exposed population is infected but not infectious. After this period, we assume that the host can naturally be partitioned to either asymptomatic (A) or presymptomatic (P). The fraction of the former is ϕ, while of the latter $1 - \phi$. While both A and P play a role (along with the infected I) in further transmitting the virus, and indeed A have been argued to play a crucial role [9, 10], it is only P that will present symptoms after an additional time scale, the preclinical period $\tau_p = 1/\sigma_2$. The incubation period, i.e., the period from infection to the development of (clinical) symptoms, for this partition $\tau_{\text{inc}} = \tau_l + \tau_p = 1/\sigma_1 + 1/\sigma_2$ is of the order of 5 days [24], and represents the time till the onset of symptoms.

From there on, the asymptomatics A continue as if nothing happened, given that they have minimal or no symptoms. Their path is only towards recovery with a characteristic rate M_{AR}, or with a time scale representing the asymptomatic infectious period $\tau^A_{\text{inf}} = 1/M_{AR}$ that is typically expected to be on the order of 7 days. This is why in most countries quarantine is expected to last around 14 days (7 days of infectiousness till recovery and another 7 till recovery of any other person that may be infected among the ones in close contact with the person of interest). In order to distinguish those recovered from asymptomatics (which cannot be directly monitored, unless extensive testing is performed in a community) from those coming from a path of symptoms/sickness (which can be –at least partially– monitored), we denote those recovered from A as A_R.

The path of the presymptomatics P is more complicated. Indeed, these may still recover (R) without the need for hospitalization and without severe manifestation of symptoms (going through class I). However, in a fraction γ of the cases hospitalization is needed. Recovery or hospitalization in the model is associated with a time scale $1/M$, the symptomatic infectious period $\tau^I_{\text{inf}} = 1/M$. Subsequent steps involve a fraction ω of the hospitalized that die, over a time scale $1/\psi$ and a fraction $1 - \omega$ that recover over a time scale $1/\chi$. The above offers an, in principle, complete description of the modeled quantities within our system. We should note that β refer to the coefficients of interaction between A (or P) and S, as well as I and S, leading to new infections; these are, respectively, β_{SA} and β_{SI}. We note here, that we somewhat abuse notation as far as β's are concerned. Namely, it is relevant consider the transmission rate $\beta = \frac{\tilde{\beta}}{N}$, where N is the total population. What we report in the tables that follow is actually $\tilde{\beta}$. In terms of the relevant time scales, the infectious period associated with symptomatically infected is $\tau^I_{\text{inf}} = 1/M$, with asymptomatic individuals $\tau^A_{\text{inf}} = 1/M_{AR}$, whereas the infectious period associated with presymptomatic individuals is $\tau^P_{\text{inf}} = \tau_p + \tau^I_{\text{inf}} = 1/\sigma_2 + 1/M$.

The transcription of the above steps in equations leads to the following ODEs:

$$
\begin{aligned}
\frac{\mathrm{d}S}{\mathrm{d}t} &= -\beta_{SA}(t)S(A+P) - \beta_{SI}(t)SI - \mu S \\
\frac{\mathrm{d}E}{\mathrm{d}t} &= \beta_{SA}(t)S(A+P) + \beta_{SI}(t)SI - \sigma_1 E \\
\frac{\mathrm{d}P}{\mathrm{d}t} &= (1-\phi)\sigma_1 E - \sigma_2 P \\
\frac{\mathrm{d}A}{\mathrm{d}t} &= \phi\sigma_1 E - M_{AR}A \\
\frac{\mathrm{d}A_{\mathrm{R}}}{\mathrm{d}t} &= M_{AR}A \\
\frac{\mathrm{d}I}{\mathrm{d}t} &= \sigma_2 P - MI \\
\frac{\mathrm{d}H}{\mathrm{d}t} &= \gamma MI - (1-\omega)\chi H - \omega\psi H \\
\frac{\mathrm{d}R}{\mathrm{d}t} &= (1-\gamma)MI + (1-\omega)\chi H \\
\frac{\mathrm{d}D}{\mathrm{d}t} &= \omega\psi H
\end{aligned}
$$

A schematic diagram of the model is shown in figure 1.

In the practical aspects of what follows, we will consider the data for Mexico, with a total population of 127,575,528 people (in 2019) and more than 430,000 confirmed cases and 47,000 deaths by the beginning of August 2020. Data were taken from "Dirección General de Epidemiología (DGE)" of "Gobierno de México" [28]. These data have the particularity of including each clinical case, from which we retrieve three basic pieces of information: the date when symptoms start, the death date (if applicable) and the age. The data are updated on a daily basis. As the way of measuring always implies an underestimation of the number of cases and deaths in the days close the report's (especially because of the delay in death communications to the DGE), we have performed fits up to dates about 20 days from the report date (i.e. the report date is July 29 and fits are performed until July 10).

medRxiv preprint doi: https://doi.org/10.1101/2020.08.11.20172833; this version posted August 14, 2020. The copyright holder for this preprint (which was not certified by peer review) is the author/funder, who has granted medRxiv a license to display the preprint in perpetuity. All rights reserved. No reuse allowed without permission.

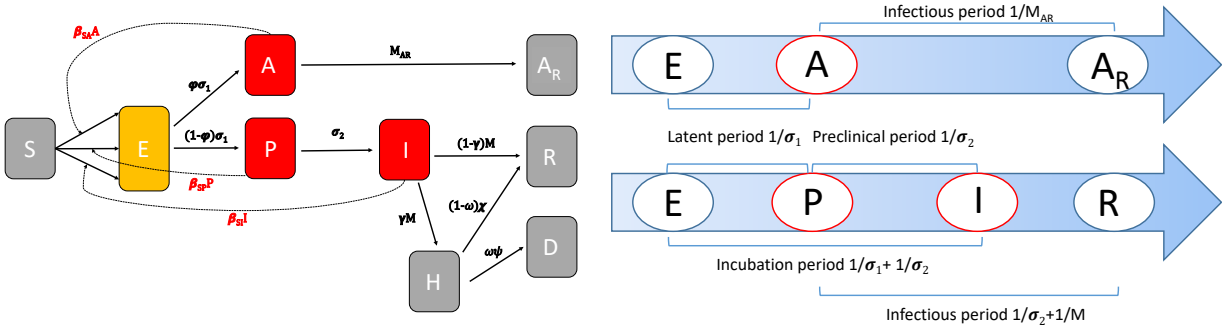

FIG. 1. Schematic diagram of the single-population model (left panel) and a diagram of the two disease progression pathways: the asymptomatic and the symptomatic one (right panel, based on a relevant variation of [8] adapted to the specific compartments and time scales of the present model).

Our principal diagnostic quantities in order to obtain the optimal parameters for the model will be the time series for deaths $D(t)$, but we will also monitor the cumulative infections. The latter in the realm of the present model amounts to $C(t) = I(t) + H(t) + R(t) + D(t)$, i.e., the sum of the individuals going through the part of the network involving the symptomatically infected. We take $t = 0$ as March 22, and fit data to July 10. This reflects our effort to be (in terms of the total numbers of both diagnostics) well within the "well mixed" regime from the beginning of the infection where the ODEs of interest are expected to be relevant.

We are particularly interested in the effect of non-pharmaceutical intervention strategies on the spreading and development of the disease. Such strategies render the transmission rates time dependent. On April 21 ($t_q = 30$) a light form of social distancing was enforced in Mexico. In addition, we will consider a number of scenarios according to which a more severe lockdown may be imposed on August 10 ($t_L = 141$).

We are particularly interested in how non-pharmaceutical intervention strategies modify the spreading and development of the disease. Such strategies render the transmission rates time dependent. On April 21 ($t_q = 30$) a light form of social distancing was enforced in Mexico. In addition, we will consider a number of scenarios according to which a more severe lockdown may have been imposed on August 10 ($t_L = 141$).

The effect of interventions on the overall transmission rate β may be estimated by considering biological and physical properties of expelled respiratory droplets, which are the carriers of the pathogens and specifically of SARS-CoV-2. The transmission rate is usually written as $\beta = cp$, with c the number of contacts per day a susceptible individual has and p the transmission probability. For pathogen transmission via infectious respiratory droplets (of diameter d), be they airborne (airborne transmission) or settled (contact transmission), the transmission rate has been expressed as, cf. Refs. [25] and [26] (for airborne transmission)

$$\beta = \beta_d \frac{\kappa_d}{\alpha_d}, \tag{1}$$

where κ_d is the respiratory droplet emission rate (viral shedding) by e.g. breathing, speaking, coughing, sneezing, α_d is the droplet effective removal rate, by e.g. gravitational settling, ambient airflow, pathogen inactivation, and β_d the transmission rate per deposited respiratory droplet. The subscript "d" refers to a specific droplet size. As we will use it Eq. (1) to *estimate* how the overall transmission rate changes we will neglect its complex dependence on d. Lastly, the droplet transmission rate β_d depends on the number of effective contacts a susceptible has with other individuals, the number of pathogens contained in an infectious droplet (its pathogen load) , and the virus transmission probability per inhaled/deposited droplet.

Social distancing, or other lockdown measures that restrict human mobility, decreases the average number of daily contacts, and possibly the average duration of contact, thereby decreasing β_d (and consequently β). In what follows we denote this fractional decrease as η_{SA} and η_{SI}. Another common intervention measure is the use of surgical face masks. Milton et al. (2013) [27] argued that their use produced a 3.4-fold reduction in viral aerosol shedding. Face masks also render physical contact of infected hands with susceptible areas on an individual's face (mouth, eyes, nose) more difficult. They, also, modify the expelled air flow, with consequential effects on droplet transport and dispersion in the environment and their airborne lifetime (thus their removal rate). We suggest that the combined effect of wearing surgical face masks is primarily conditioned by the decrease in viral shedding. We, thus, estimate that their use (if the whole population used them continuously and correctly fitted) would decrease the overall transmission rate to $\sim 0.2\beta$.

The effect of lockdown measures is modelled herein by the parameter ζ, Eq. (2): we set the after lockdown transmission rate to be $\zeta\beta$. This parameter incorporates the effect of all lockdown measures, including the requirement that face mask be worn. As the previous estimate leads to a considerable decrease in the transmission rate, we decided to be conservative and we varied ζ from 1.0 to 0.5.

medRxiv preprint doi: https://doi.org/10.1101/2020.08.11.20172833; this version posted August 14, 2020. The copyright holder for this preprint (which was not certified by peer review) is the author/funder, who has granted medRxiv a license to display the preprint in perpetuity. All rights reserved. No reuse allowed without permission.

These features should be kept in mind, as we aim not only to capture the current trend of the pandemic, but also to suggest mitigation strategies that may reduce the cumulative infections, as well as the fatalities as a result of COVID-19 in the time series of interest, namely in the case of Mexico. In what follows, we suggest possible scenarios of social distancing, and we accordingly evaluate their impact as regards the potential reduction induced in the number of deaths and cumulative infections for the time series of interest that is obtained from the DGE data.

To explore the impact of *further* lockdown effects to mitigate the spread of the infection, we will consider the following time dependence for the β's:

$$\begin{aligned}\beta_{SI}(t) =& \beta_{SI}\left[\eta_{SI} + (1-\eta_{SI})\frac{1-\tanh[2(t-t_q)]}{2}\right] \\ \beta_{SA}(t) =& \beta_{SA}\left[\eta_{SA} + (1-\eta_{SA})\frac{1-\tanh[2(t-t_q)]}{2} + \eta_{SA}(\zeta-1)\frac{1+\tanh[2(t-t_L)]}{2}\right]\end{aligned} \tag{2}$$

with $0 < \zeta \leq 1$, as argued, and t_q, t_L previously specified. For $\zeta = 1$, Eqs. (2) reduce to the equations modelling the decrease in the number of personal contacts when a light form of social distancing is imposed (no lockdown, no requirement to wear face masks). Figure 2 shows the time-dependence of the β's. The first jump in the value of β_{SI} and β_{SA} (i.e., the transmission rates to infected and presymptomatic-asymptomatic virus carriers) occurs at t_q. The next jump occurs at t_L and is assumed to take place only for the presymptomatic or asymptomatic carriers of the virus through the imposition of lockdown restrictions at $t = t_L$.

As our data will show below, the growth of fatalities as well as infections in the country is considerable and thus our model suggests the relevance of the application of significant lockdown restrictions so that the progress of the infection be substantially curbed.

In the parameters of the single-population model, we assume the following constraints:

- $\eta_{SI} \leq 1$
- $\eta_{SA} \leq 1$
- $5 \leq 1/\sigma_1 + 1/\sigma_2 \leq 6$

The first two are rather trivial (and without loss of generality) implying that we go from a value of the transmission rate β, to a lower value $\beta \times \eta$ in both the interactions of S with A (or P) and in those of S with I. The third constraint is based on observations associated with SARS-CoV-2 [24] positioning the incubation period associated with this virus between roughly 5 and 6 days from the start of exposure.

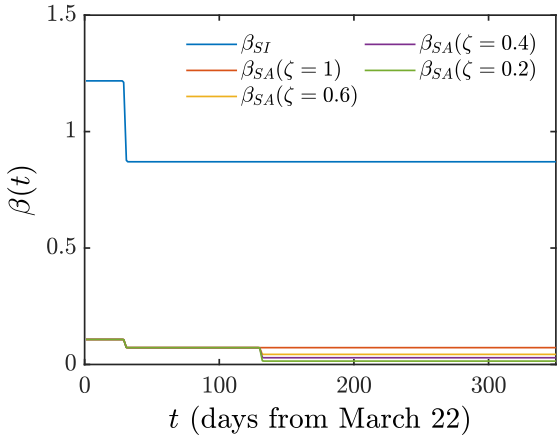

FIG. 2. Single-population model. Transmission-rate time dependence (β_{SI} and β_{SA}). For the asymptomatic carriers of the virus the transmission rate, which initially decreases due to social distancing (reflected in η_{SA}) is further assumed to decrease by a factor ζ (shown for different cases), reflecting the effect of obligatory wearing of (effective) face masks or other lockdown-based decrease of contacts. For the infected population instead, we assume that β_{SI} decreases only once due to social distancing, (η_{SI}), but it does not further decrease, given the self-isolation of such individuals due to the presence of symptoms.

medRxiv preprint doi: https://doi.org/10.1101/2020.08.11.20172833; this version posted August 14, 2020. The copyright holder for this preprint (which was not certified by peer review) is the author/funder, who has granted medRxiv a license to display the preprint in perpetuity. All rights reserved. No reuse allowed without permission.

B. Results

We now present the results determined by an optimization procedure that identifies under the above minimal constraints the optimal parameters of the model in comparison to the time series of data obtained from the Government of Mexico [28]. Table I shows the optimal parameters found from minimizing the norm

$$\mathcal{N} = \sum_i \Big(\alpha_1 |\log(C_{\rm num}(t_i)) - \log(C_{\rm obs}(t_i))| + \alpha_2 |\log(D_{\rm num}(t_i)) - \log(D_{\rm obs}(t_i))| \Big) \tag{3}$$

with $\alpha_1 = 0$, $\alpha_2 = 1$ as displayed in Fig. 3. We will compare these results shortly with the case of $\alpha_1 = \alpha_2 = 0.5$ shown in Fig. 4. The rationalization of these two choices is as follows. In the former case, we take the view that the only "ground truth" data is that of the deaths; in fact, even those can be under-estimated (deaths with "suspicion" of COVID-19, but no definitive test) or –perhaps less likely– over-estimated (deaths attributed to COVID-19 without explicit testing), but here we will assume that this is the most well-defined piece of data, as is generally expected to be the case. On the other hand, infections are broadly expected to be under-reported. This is because many of the cases with symptoms do not get to be serious enough to lead to hospitalization or to be reported. In that light, it is expected that assuming the deaths as ground truth, we should expect to find a significant over-estimation of the number of infections (we return to this point below). If, on the other hand, we "force" the model to match the current reporting of infections, then we will end up with a better approximation "on average" to both curves but with a potential adverse by-product in the resulting number of deaths that we will discuss below. This will be due, in addition, to issues of measurement errors in the setting of cumulative incidences, as discussed, e.g., in [29].

Our observation in Fig. 3 is that the model can provide an excellent fit to the total number of deaths, but in that case, there is a considerable over-prediction of the number of infections, presumably because numerous of the incurred infections are not reported in the official data. The results can be compared with Fig. 4 where both deaths and cumulative infections are attempted to be fitted, i.e., $\alpha_1 = \alpha_2$ in the minimization procedure above. Here, we see that while the model is capable of doing a very adequate job in following $C(t)$, it also does a reasonable job of capturing $D(t)$. *Nevertheless*, there is a caveat to the latter. A closer observation of the semilogarithmic scale of the graph will lead the astute reader to observe that as the model is trying to juggle the optimization of both time-series, it slightly over-predicts deaths early on, slightly under-predicts them at the middle of the time series and eventually slightly overpredicts again at longer times, likely predicting a much more catastrophic scenario (with multiple hundreds of thousands of deaths at the end of the examined evolution) than is warranted by the data trends. For this reason, we will stick to the consideration of the former case of Fig. 3 hereafter.

Before we discuss the implications of mitigation strategies, let us briefly comment on the optimal parameter values identified by the model, as illustrated in Table I. The latent period $1/\sigma_1$ is indeed found to be in the vicinity of 3 days (2.8765), while the total incubation period is comfortably within the prescribed interval of 5-6 days ($1/\sigma_1 + 1/\sigma_2 \approx 5.3836$). The time scale of recovery for asymptomatics is a little under 7 days as expected ($1/M_{AR} = 6.0983$), while the time scale of going from symptomatic infected to hospitalization is close to 4 days which is also fairly reasonable ($1/M = 3.6221$). The model predicts a large fraction of asymptomatics ($\phi = 0.8134$) which is in line with discussions such as that of [10]. However, such results should be taken with a grain of salt. This is because of issues associated with the notion of identifiability [30]. In particular, a systematic analysis of the model in connection to identifiability (the formal mathematical details of which are outside the scope of the present work) suggest that ϕ itself will not end up being an identifiable parameter, but rather the product of ϕ with β's will be on such. As a result, we do not significantly focus on the larger value obtained for ϕ, but we do note it. Interestingly, the model predicts that roughly 30% of those symptomatically infected need hospitalization, while the rest recover. Of those hospitalized, nearly 30% result in fatalities, leading to a death percentage of about 10% among those that present symptoms. Indeed, this is a rather significant fatality percentage accounting for the large number of deaths in the population. The average time scale of recovery upon hospitalization is about 10.7 days ($1/\chi$), while that of death ($1/\psi$) is found to optimally be near 11.5 days. However, here too we should highlight that ω and ψ are not independently identifiable (only their product is) and neither is $(1-\omega)$ and χ (again only their product is). Hence, the relevant optimization parameter values should be considered as coming together with the corresponding caveats (and the relevant products as being the genuine model derived quantities), despite their realistic individual values. It is relevant to note that at the initial time of the model, it is not known how many members of the population are exposed, asymptomatic or presymptomatic. We thus optimize those parameters too, obtaining the last 3 entries of the Table.

Our aim is now to explore the impact of mitigating measures reducing the obtained optimal case by a factor of $\zeta < 1$ ($\zeta = 1$ is the current optimization result without additional measures). Table II summarizes the results of Fig. 5, in which the predictions for $\zeta = 0.9, 0.7, 0.5$ are displayed. It can be seen that a decrease of β by a factor between 0.9 and 0.5 could have a *catalytic* result as concerns the predictions of the model both for the deaths and as regards the cumulative infections. In particular, a decrease of ζ by a factor of even as little as 0.9 will reduce the number of deaths by more than 800, only within the time frame between August 10 and September 10, while a decrease by a factor of $1/2$ is predicted within this single population model to save close to 4000 lives in this interval alone. The corresponding effect to the number of infections is perhaps even more striking (also accounting for the fact that many of these infections could lead to fatalities at a later stage). In particular, a decrease of ζ to 0.9 leads to about 24000 less infections, while to a factor of $1/2$ would lead to about 100000 less infections again just within

medRxiv preprint doi: https://doi.org/10.1101/2020.08.11.20172833; this version posted August 14, 2020. The copyright holder for this preprint (which was not certified by peer review) is the author/funder, who has granted medRxiv a license to display the preprint in perpetuity. All rights reserved. No reuse allowed without permission.

TABLE I. Optimal parameters for the single population model. For a discussion thereof, see the text.

Parameter	Symbol	Optimal value	Parameter	Symbol	Optimal value
Transmission rate [per day]	β_{SI}	1.4789	Infectivity period (A) [days] τ_{inf}^{A}	$1/M_{\text{AR}}$	6.0983
Transmission rate [per day]	β_{SA}	0.1982	Conversion fraction (I to H, R)	γ	0.2991
Social distancing effect	η_{SI}	0.5806	Conversion fraction (H to R, D)	ω	0.3095
Social distancing effect	η_{SA}	0.4585	Recovery period(H to R) [days]	$1/\chi$	10.6927
Latent period [days] τ_l	$1/\sigma_1$	2.8765	H to D period [days]	$1/\psi$	11.5331
Preclinical period [days] τ_p	$1/\sigma_2$	2.5071	Initial population fraction (E)	$E(0)/I(0)$	2.0851
A/P partitioning	ϕ	0.8134	Initial population fraction (A)	$A(0)/I(0)$	2.0532
Infectivity period (I) [days] τ_{inf}^{I}	$1/M$	3.6221	Initial population fraction (P)	$P(0)/I(0)$	0.5462

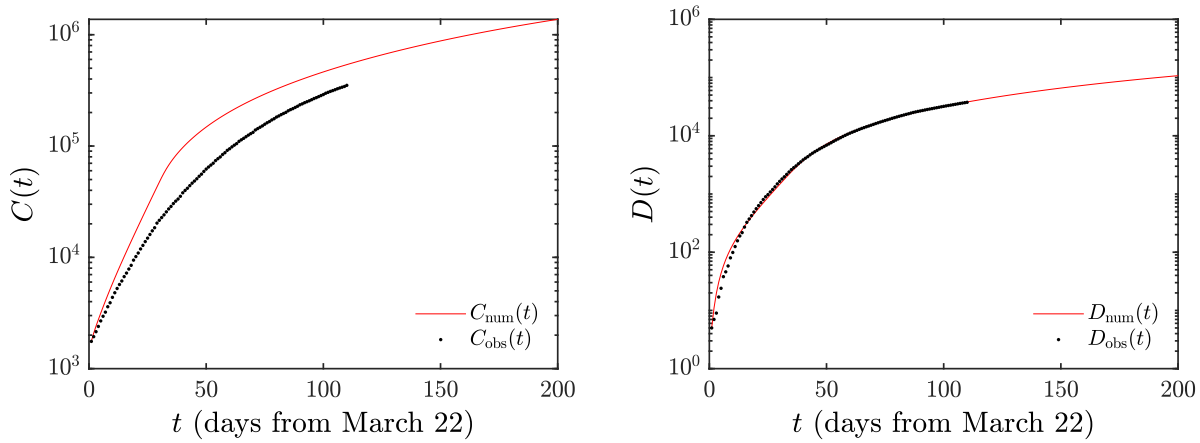

FIG. 3. Single-population model. Number of cases $C(t)$ (left) and of deaths $D(t)$ (right) found by minimizing norm (3) with $\alpha_1 = 0$ and $\alpha_2 = 1$. To produce the fit we have used the data until July 10. The prediction of the optimized model is shown by the solid line, while the official time series [28] is given by dots.

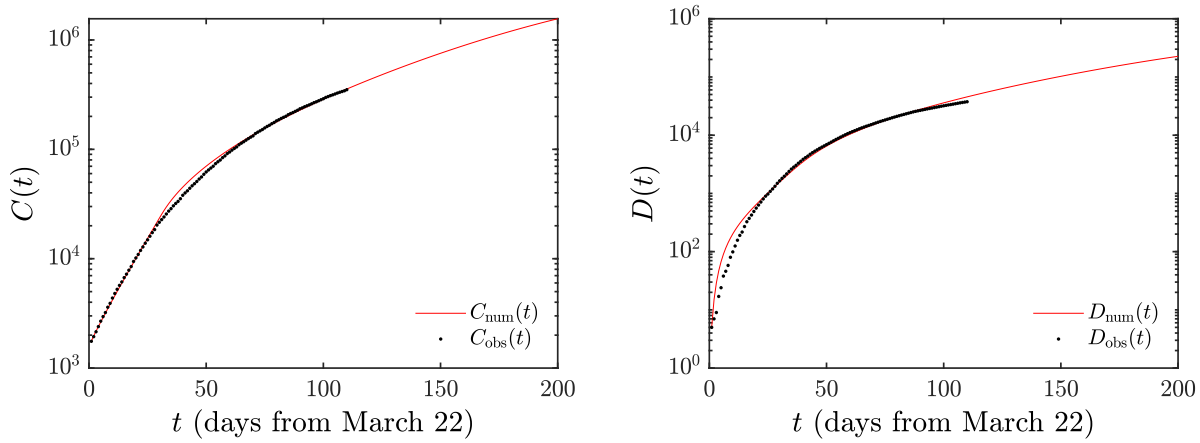

FIG. 4. As in the previous figure, but for $\alpha_1 = \alpha_2$. The number of cases $C(t)$ is captured significantly better, but the lower accuracy in capturing $D(t)$ and its implications are further discussed in the text.

this 31-day period. One can clearly see the significant potential impact of further lockdown measures, a feature that may be worthwhile to factor into further public health considerations.

medRxiv preprint doi: https://doi.org/10.1101/2020.08.11.20172833; this version posted August 14, 2020. The copyright holder for this preprint (which was not certified by peer review) is the author/funder, who has granted medRxiv a license to display the preprint in perpetuity. All rights reserved. No reuse allowed without permission.

TABLE II. Single-population model. Predictions for C and D at September 10 if lockdown measures had been applied on August 10.

	$\zeta = 1$	$\zeta = 0.9$	$\zeta = 0.7$	$\zeta = 0.5$
C (total)	1090578	1066436	1024199	988931
C (from Aug. 10)	292666	268524	226289	191022
D (total)	83593	82744	81203	79848
D (from Aug. 10)	24362	23514	21972	20617

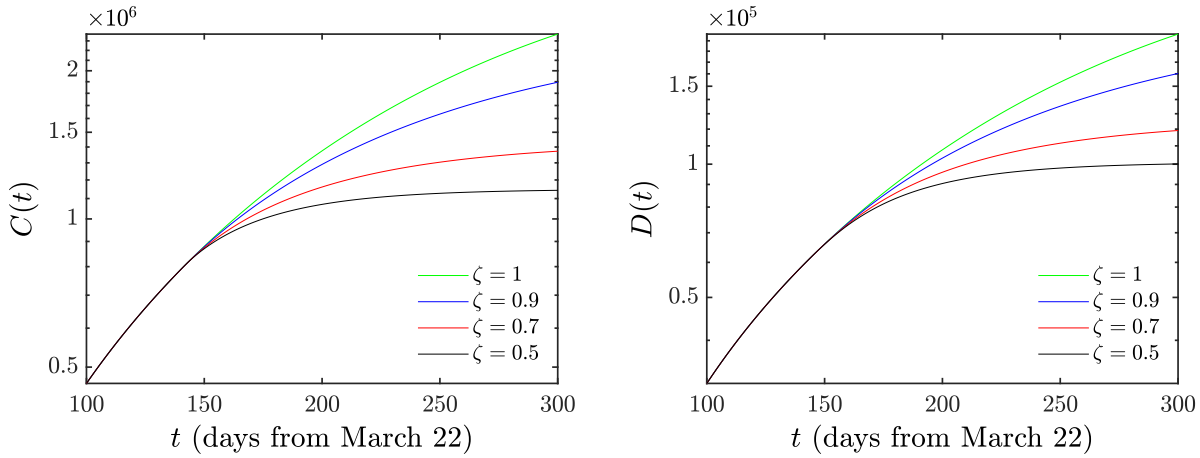

FIG. 5. Single-population model. Evolution of the number of cases (left) and of deaths (right) for different ζ if lockdown had been applied on August 10 ($t = 141$). Notice the significant curbing of the pandemic as a result of such intervention measures, especially so at the level of long term effects in the case of $\zeta = 0.7$ and $\zeta = 0.5$.

As our final comment about the single population variant of the model, we note that an important quantity in epidemiological models of this general type is the notion of the basic reproductive number R_0; see, e.g., [3]. The number effectively represents the expected new infections (so-called secondary infections) from a single infection in a population where all subjects are susceptible. Using the so-called next-generation approach [31], we can determine the basic reproductive number on the basis of the parameters of the model and the susceptible population [see the Appendix for details], according to the expression:

$$R_0 = \left[\frac{\beta_{SA}(1-\phi)}{\sigma_2} + \frac{\beta_{SA}\phi}{M_{AR}} + \frac{\beta_{SI}(1-\phi)}{M} \right] S^* \,, \tag{4}$$

with S^* the initial susceptible population, namely $S^* = 1$ as parameters β are normalized by N, as discussed above. For the parameters in Tab. I, one obtains a value of $R_0 = 2.0755$. The effective reproductive number at the beginning of social distancing measures ($t = t_q$) is $R_e = 1.5745$ which is unable to mitigate the pandemic effects. In order that $R_e < 1$, it is needed that ζ is smaller than 0.8506. That is why among the case examples that we considered, those with $\zeta = 0.7$ and 0.5 present a significant decrease in the number of deaths not only imminently (i.e., within the interval of August 10 to September 10) but also over the longer scale prediction of Fig. 3.

III. TWO-POPULATION MODEL

A. Equations

We now turn to the two-population variant of the model. Recall that due to the different structural characteristics of the two populations as considered herein, namely below and above 65 years, we expect that this model will be more adequate in capturing both the deaths and the cumulative infections of the full population. This is because on the one hand, the younger population in our considerations is more active (belonging typically in the workforce), hence carries a different number of contacts. On the other hand, the older population has its own vulnerabilities to the impact of the virus SARS-CoV-2 and the associated disease,

medRxiv preprint doi: https://doi.org/10.1101/2020.08.11.20172833; this version posted August 14, 2020. The copyright holder for this preprint (which was not certified by peer review) is the author/funder, who has granted medRxiv a license to display the preprint in perpetuity. All rights reserved. No reuse allowed without permission.

namely COVID-19. On the other hand, as explained in the Introduction, the prevalence of various risk factors within the Mexican population [22] render this partition even more relevant to consider towards capturing the detailed data trends.

Firstly, we discuss the mathematical structure of the model. Here, we basically assume that each of the populations has its own set of parameters. Thus, the superscript y will denote the parameters associated with the younger population, while the superscript o will be connected to the older population. Naturally, the number of variables (S, E, A, P, I, H, R, D) now doubles with each part having a younger and an older component. It is worthwhile that for some quantities that are associated with the virus, such as σ_1 and σ_2, characterizing the latent and incubation time thereof, we assume these to be independent of age. Lastly, we explore a *mildly anisotropic* variant of the model where in terms of the interactions $\beta^o \equiv \beta^{oy} = \beta^{yo} = \beta^{oo}$ and $\beta^y \equiv \beta^{yy}$. That is to say, we assume that the older population has a different interaction within itself and with the younger individuals, than the younger members of the population between themselves [18]. This is a reasonable assumption under the present conditions where the more sensitive older members of the population are advised to reduce their interactions. While, in principle, we could have used a fully anisotropic variant of the model, we find it relevant to attempt to reduce the overall number of model parameters, hence the above choice.

$$
\begin{aligned}
\frac{\mathrm{d}S^y}{\mathrm{d}t} &= -\beta^{yy}_{SI}(t)S_yI_y - \beta^{yy}_{SA}(t)S_y(A_y+P_y) - \beta^{yo}_{SI}(t)S_yI_o - \beta^{yo}_{SA}(t)S_y(A_o+P_o)\\
\frac{\mathrm{d}E^y}{\mathrm{d}t} &= -\sigma_1E_y + \beta^{yy}_{SI}(t)S_yI_y + \beta^{yy}_{SA}(t)S_y(A_y+P_y) + \beta^{yo}_{SI}(t)S_yI_o + \beta^{yo}_{SA}(t)S_y(A_o+P_o)\\
\frac{\mathrm{d}P^y}{\mathrm{d}t} &= (1-\phi^y)\sigma_1E_y - \sigma_2P^y\\
\frac{\mathrm{d}A^y}{\mathrm{d}t} &= \phi^y\sigma_1E_y - M^y_{\mathrm{AR}}A^y\\
\frac{\mathrm{d}A^y_{\mathrm{R}}}{\mathrm{d}t} &= M^y_{\mathrm{AR}}A^y\\
\frac{\mathrm{d}I^y}{\mathrm{d}t} &= \sigma_2P^y - M^yI^y\\
\frac{\mathrm{d}H^y}{\mathrm{d}t} &= \gamma^yM^yI^y - (1-\omega^y)\chi^yH^y - \omega^y\psi^yH^y\\
\frac{\mathrm{d}R^y}{\mathrm{d}t} &= (1-\gamma^y)M^yI^y + (1-\omega^y)\chi^yH^y\\
\frac{\mathrm{d}D^y}{\mathrm{d}t} &= \omega^y\psi^yH^y\\
\frac{\mathrm{d}S^o}{\mathrm{d}t} &= -\beta^{oo}_{SI}(t)S_oI_o - \beta^{oo}_{SA}(t)S_o(A_o+P_o) - \beta^{oy}_{SI}(t)S_oI_y - \beta^{oy}_{SA}(t)S_o(A_y+P_y)\\
\frac{\mathrm{d}E^o}{\mathrm{d}t} &= -\sigma_1E_o + \beta^{oo}_{SI}(t)S_oI_o + \beta^{oo}_{SA}(t)S_o(A_o+P_o) + \beta^{oy}_{SI}(t)S_oI_y + \beta^{oy}_{SA}(t)S_o(A_y+P_y)\\
\frac{\mathrm{d}P^o}{\mathrm{d}t} &= (1-\phi^o)\sigma_1E_o - \sigma_2P^o\\
\frac{\mathrm{d}A^o}{\mathrm{d}t} &= \phi^o\sigma_1E_o - M^o_{\mathrm{AR}}A^o\\
\frac{\mathrm{d}A^o_{\mathrm{R}}}{\mathrm{d}t} &= M^o_{\mathrm{AR}}A^o\\
\frac{\mathrm{d}I^o}{\mathrm{d}t} &= \sigma_2P^o - M^oI^o\\
\frac{\mathrm{d}H^o}{\mathrm{d}t} &= \gamma^oM^oI^o - (1-\omega^o)\chi^oH^o - \omega^o\psi^oH^o\\
\frac{\mathrm{d}R^o}{\mathrm{d}t} &= (1-\gamma^o)M^oI^o + (1-\omega^o)\chi^oH^o\\
\frac{\mathrm{d}D^o}{\mathrm{d}t} &= \omega^o\psi^oH^o
\end{aligned}
\tag{5}
$$

In a natural extension of what we assumed for the fitting of the single population model, we assume that as a result of the

medRxiv preprint doi: https://doi.org/10.1101/2020.08.11.20172833; this version posted August 14, 2020. The copyright holder for this preprint (which was not certified by peer review) is the author/funder, who has granted medRxiv a license to display the preprint in perpetuity. All rights reserved. No reuse allowed without permission.

partial measures already in place, the value of each of the β's has a temporal variation of the form:

$$\begin{aligned}\beta^y(t) =&\beta^y\left[\eta^y + (1-\eta^y)\frac{1-\tanh[2(t-t_q)]}{2}\right],\\ \beta^o(t) =&\beta^o\left[\eta^o + (1-\eta^o)\frac{1-\tanh[2(t-t_q)]}{2}\right].\end{aligned} \tag{6}$$

This implies that each of the β's (associated with younger or older populations) has been reduced by a respective factor of η (with the corresponding superscript).

Again, extending the respective constraints (without loss of generality for the η's) to each population, as well as the incubation time expectation, we impose the following conditions on the proposed optimization.

- $\eta^y_{SI} \leq 1$
- $\eta^y_{SA} \leq 1$
- $\eta^o_{SI} \leq 1$
- $\eta^o_{SA} \leq 1$
- $5 \leq 1/\sigma_1 + 1/\sigma_2 \leq 6$

Recall that part of our motivation involves the intention to consider the impact of potential measures in the form of social distancing and the associated reduction of contacts (as well as the additional use of protective measures such as face masks etc.). In that light, for each of the two populations, we assume again that the infected members maintain (in their quarantine) their β's, while the circulating asymptomatic individuals would be affected by these measures through a further reduction of their β's by factors ζ^y and ζ^o. The associated temporal dependence of the transmission rate factors then reads:

$$\begin{aligned}\beta^y_{SI}(t) =&\beta^y_{SI}\left[\eta^y_{SI} + (1-\eta^y_{SI})\frac{1-\tanh[2(t-t_q)]}{2}\right]\\ \beta^o_{SI}(t) =&\beta^o_{SI}\left[\eta^o_{SI} + (1-\eta^o_{SI})\frac{1-\tanh[2(t-t_q)]}{2}\right]\\ \beta^y_{SA}(t) =&\beta^y_{SA}\left[\eta^y_{SA} + (1-\eta^y_{SA})\frac{1-\tanh[2(t-t_q)]}{2} + \eta^y_{SA}(\zeta^y-1)\frac{1+\tanh[2(t-t_L)]}{2}\right]\\ \beta^o_{SA}(t) =&\beta^o_{SA}\left[\eta^o_{SA} + (1-\eta^o_{SA})\frac{1-\tanh[2(t-t_q)]}{2} + \eta^o_{SA}(\zeta^o-1)\frac{1+\tanh[2(t-t_L)]}{2}\right]\end{aligned} \tag{7}$$

Figure 6 shows the time-dependence of the β's. This Figure is dedicated to the scenario in which *only* the old population is required to adhere to the additional restrictive measures (suggested to be imposed as of August 10), i.e. $\zeta^y = 1$ and $\zeta^o \equiv \zeta$. This is intended to explore the mitigation of contacts within the older population alone. This approach has been argued in other cases to be a reasonably safe approach towards attempting to return to economic and social stability [32]. Later, we will explore the possibility of lockdown measures imposed on both older and younger populations. The latter will be more relevant to compare with the single population results of the previous section.

Once again, the optimal parameters can be found through our optimization procedure stemming from minimizing the norm

$$\begin{aligned}\mathcal{N} = \sum_i \Big(&\alpha_1\left[|\log(C^y_{\rm num}(t_i)) - \log(C^y_{\rm obs}(t_i))| + |\log(C^o_{\rm num}(t_i)) - \log(C^o_{\rm obs}(t_i))|\right] +\\ &\alpha_2\left[|\log(D^y_{\rm num}(t_i)) - \log(D^y_{\rm obs}(t_i))| + |\log(D^o_{\rm num}(t_i)) - \log(D^o_{\rm obs}(t_i))|\right]\Big)\end{aligned} \tag{8}$$

with $\alpha_1 = 0$, and $\alpha_2 = 1$ as displayed in Fig. 7. The optimal parameters in this case for the two population model are given in Table III. We have also performed the optimization for $\alpha_1 = \alpha_2$, finding (results not shown here for brevity) that it bears similar advantages (such as capturing more adequately $C(t)$ and similar pathologies such as the overestimation of deaths, most notably in the younger population, but also in the older population).

We can observe by comparing the optimal coefficients of the model that the nature of the data for the two populations (older and younger) leads to a corresponding selection of the optimization coefficients so that some suitable inequalities arise. In particular, it is evident for the data of Table III that the transmission rates are considerably higher both for asymptomatic (presymptomatic) and also for infected individuals in the older population, in comparison to the younger one. The model predicts a comparable fraction of asymptomatics within the two populations, although again given the issues of identifiability, we do not assign any special weight to this observation. We can see that also within the symptomatic component of the respective generations, the

medRxiv preprint doi: https://doi.org/10.1101/2020.08.11.20172833; this version posted August 14, 2020. The copyright holder for this preprint (which was not certified by peer review) is the author/funder, who has granted medRxiv a license to display the preprint in perpetuity. All rights reserved. No reuse allowed without permission.

TABLE III. Optimal parameters for the two populations model.

Parameter	Symbol	Optimal value	Parameter	Symbol	Optimal value
Transmission rate (y) [per day]	β^y_{SI}	0.9171	Infectivity period (A, y)	$1/M^o_{\rm AR}$	5.9498
Transmission rate (y) [per day]	β^y_{SA}	0.1116	Conversion factor (I to H, R, y)	γ^y	0.2682
Transmission rate (o) [per day]	β^o_{SI}	1.3861	Conversion factor (I to H, R, o)	γ^o	0.6239
Transmission rate (o) [per day]	β^o_{SA}	0.5157	Conversion factor (H to R,D, y)	ω^y	0.0958
Social distancing effect (y)	η^y_{IS}	0.5100	Conversion factor (H to R,D, o)	ω^o	0.3479
Social distancing effect (y)	η^y_{AS}	0.2521	Recovery period (H to R, y)	$1/\chi^y$	11.8431
Social distancing effect (o)	η^o_{IS}	0.7377	Recovery period (H to R, o)	$1/\chi^o$	12.1310
Social distancing effect (o)	η^o_{AS}	0.5873	H to D period y	$1/\psi^y$	9.3985
Latent period τ_l	$1/\sigma_1$	2.9958	H to D period o	$1/\psi^o$	12.7025
Preclinical period τ_p	$1/\sigma_2$	2.2293	Initial population fraction (E, y)	$E^y(0)/I^y(0)$	2.6034
A/P partitioning (y)	ϕ^y	0.5553	Initial population fraction (E, o)	$E^o(0)/I^o(0)$	2.2670
A/P partitioning (o)	ϕ^o	0.5502	Initial population fraction (A, y)	$A^y(0)/I^y(0)$	2.3085
Infectivity period (I, y)	$1/M^y$	3.1513	Initial population fraction (A, o)	$A^o(0)/I^o(0)$	2.1822
Infectivity period (I, o)	$1/M^o$	4.0695	Initial population fraction (P, y)	$P^y(0)/I^y(0)$	0.8474
Infectivity period (A, y)	$1/M^y_{\rm AR}$	5.5263	Initial population fraction (P, o)	$P^o(0)/I^o(0)$	0.5596

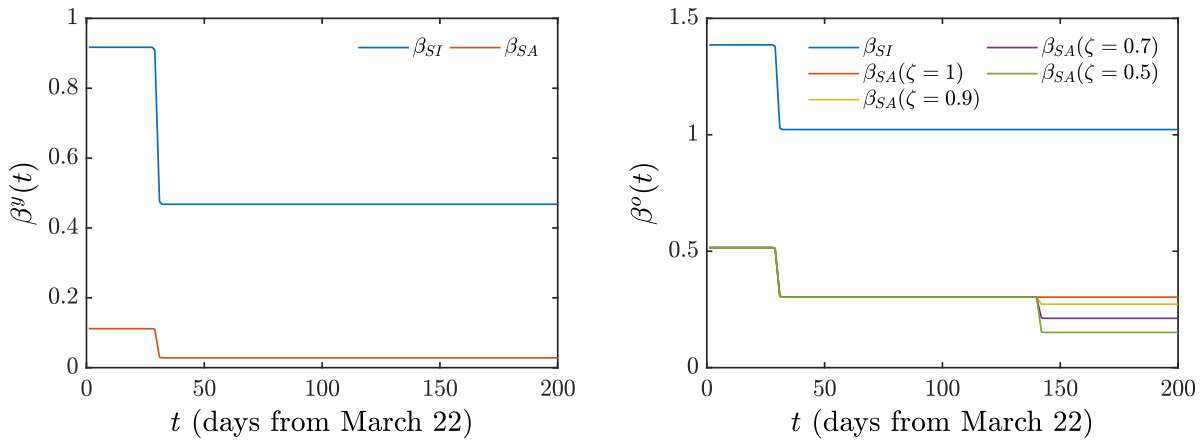

FIG. 6. Two-population model: Time dependence of β_{SI} and β_{SA} under the existing policy ($\zeta = 1$) and under the effect of additional (suggested) lockdown measures when they are applied to the older (than 65) population, i.e. $\zeta^o = 1$ and $\zeta^y \equiv \zeta$.

younger population has a far smaller γ signifying a far smaller fraction of individuals that are symptomatically infected and need hospitalization, in comparison to the older population. Similarly, the fraction among those hospitalized that are led towards fatalities is more than triple in the older population in comparison to the younger one (i.e., comparing the respective values of ω). Once again though, we do highlight that one should not really interpret ω and ψ separately, but only the product thereof (which is still significantly larger for the older population) and similarly not consider $(1-\omega)$ and χ separately but once again their product which suggests a significantly larger recovery rate for the younger population.

We now turn to the comparison of the implications of maintaining $\zeta = 1$ (i.e., the current policy) vs. the projection upon a reduction of ζ by a factor of 0.9 to 0.5 as before. The relevant results can be found in Table IV and Fig. 8. It is evident from these data that a corresponding reduction of the ζ factor by means of social distancing or lockdown measures is predicted by the model to reduce the number of infections by anywhere between nearly 16 to about 75 thousand in the two respective cases. The respective projected implications in the loss of human life range from about 400 (in the former case) to over 1800 people (in the latter case) in this interval of a month. Clearly, the projection of the model, both for the specific interval of August 10 to September 10 that is specifically monitored, but also over the longer time scale presented in Fig. 8 seem to warrant the consideration of such measures, to the degree possible.

Let us now touch upon the case where the relevant measures are applied to both populations. The corresponding variation of

medRxiv preprint doi: https://doi.org/10.1101/2020.08.11.20172833; this version posted August 14, 2020. The copyright holder for this preprint (which was not certified by peer review) is the author/funder, who has granted medRxiv a license to display the preprint in perpetuity. All rights reserved. No reuse allowed without permission.

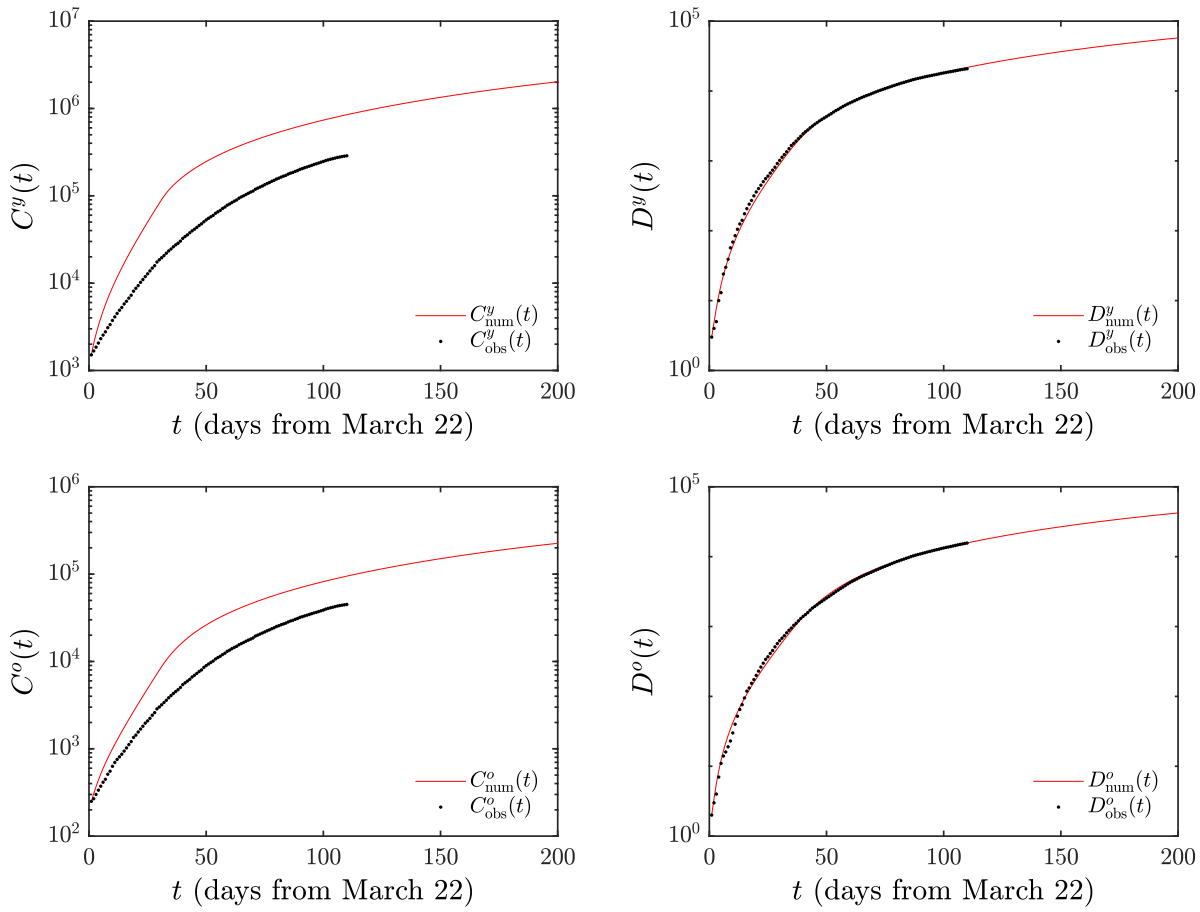

FIG. 7. Two-population model: number of cases (left) and of deaths (right) found by minimizing norm (8). The younger (than 65 years of age) population is shown in the top panels and the older (than 65) one in the bottom panels. While the corresponding fatalities are somewhat comparable, recall that there is a far more significant susceptible population in the former category in comparison to the latter one.

the β's involving an equal restrictive factor of ζ in the contacts (or related social distancing measures) for both young and old populations is shown in Fig. 6. In turn, the TableV shows the effect on both deaths and cumulative infections of these restrictive measures applied equally to both populations (this can also be compared to Table II where this was applied to the single-age, full population model). This is for the period from August 10 to September 10, i.e., for an interval of one month. Figure 10 presents a longer time scale perspective of these mitigation effects, extending well past September 10. Finally, a complementary view of the potential effect of measures can be observed in Fig. 11. Here the number of potentially fewer deaths as predicted by the model is presented both in the case of the single age model, as well as in that of the two-age model, both for restriction of just the older population (red curve) and for that of older and younger populations (blue curve). It can generally be seen that the structured form of the two population models predicts fewer avoided deaths in comparison to the less structured one-age mode. More concretely, from the Table V, we notice that within the month of interest (August 10 to September 10), the decrease in infections is by around 22000 for $\zeta = 0.9$ or by close to 100000 for $\zeta = 0.5$. These numbers are comparable to the ones of the single age model. However, as concerns the number of deaths the situation is less promising as the decrease in number of deaths over the same time frame is by less than 500 for $\zeta = 0.9$, while for $\zeta = 0.5$, the decrease in deaths is by 2174, i.e., well below the single population prediction. Nevertheless, these predictions of the model and comparisons between the restrictive measures for a single (older) population group vs. ones for the entire population, we hope may be informative towards imminent public health considerations.

We also calculated R_0 for the two-population version of our model. In this case,

$$R_0 = \frac{R_0^{yy} + R_0^{oo}}{2} + \frac{\sqrt{(R_0^{yy} - R_0^{oo})^2 + 4R_0^{yo}R_0^{oy}}}{2}, \tag{9}$$

where the explicit expressions of R_0^{ij}, $i, j = o, y$ are the given in the Appendix. We note, however, that R_0^{oo}, R_0^{yy} are identical

medRxiv preprint doi: https://doi.org/10.1101/2020.08.11.20172833; this version posted August 14, 2020. The copyright holder for this preprint (which was not certified by peer review) is the author/funder, who has granted medRxiv a license to display the preprint in perpetuity. All rights reserved. No reuse allowed without permission.

TABLE IV. Two-population model. Predictions for C and D at September 10 for parameters found by fitting the norm (8) and measures are applied to the older (than 65) population, i.e. $\zeta^o = 1$ and $\zeta^y \equiv \zeta$

	$\zeta = 1$	$\zeta = 0.9$	$\zeta = 0.7$	$\zeta = 0.5$
C^y (total)	1636390	1622367	1596586	1573602
C^o (total)	182999	180362	175457	170997
$C^y + C^o$ (total)	1819389	1802729	1772043	1744599
C^y (from Aug. 10)	410217	396194	370414	347431
C^o (from Aug. 10)	45658	43022	38116	33657
$C^y + C^o$ (from Aug. 10)	455875	439215	408530	381087
D^y (total)	45538	45370	45054	44766
D^o (total)	33451	33231	32813	32421
$D^y + D^o$ (total)	78989	78601	77867	77187
D^y (from Aug. 10)	12495	12326	12010	11722
D^o (from Aug. 10)	9277	9057	8639	8247
$D^y + D^o$ (from Aug. 10)	21771	21383	20649	19969

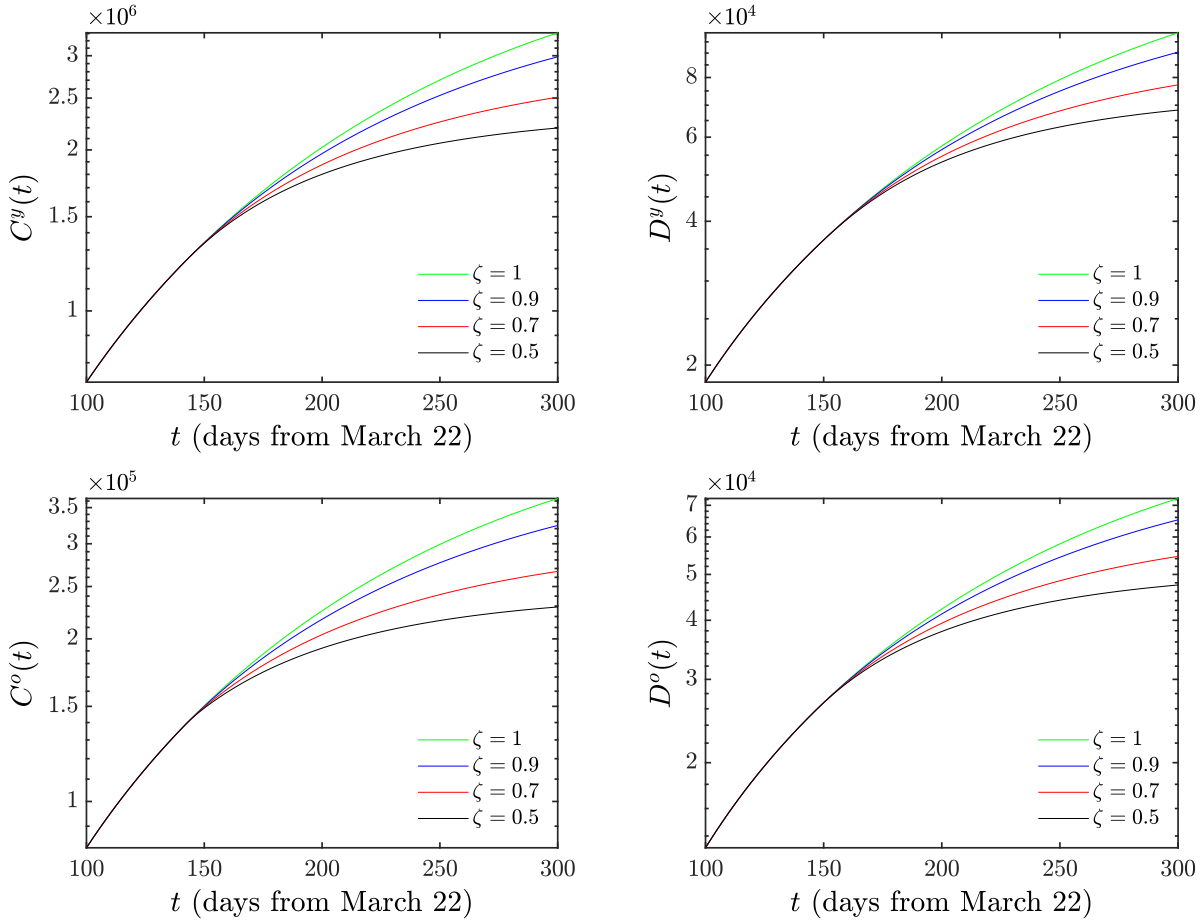

FIG. 8. Same as Fig. 5 but for the two-population model when measures are applied to the older (than 65) population, i.e. $\zeta^y = 1$ and $\zeta^o \equiv \zeta$. Notice the significant deviation of both the number of infections (left) and of the number of deaths (right), both for the younger (than 65) population and for the older (than 65) one between the current policy ($\zeta = 1$) and the suggested social-distanced (by a factor of 0.5 to 0.9) in the cases shown.

to (4) in the case when the old and young groups, respectively, are isolated. R_0^{yo} (R_0^{oy}) correspond to the case when the young

medRxiv preprint doi: https://doi.org/10.1101/2020.08.11.20172833; this version posted August 14, 2020. The copyright holder for this preprint (which was not certified by peer review) is the author/funder, who has granted medRxiv a license to display the preprint in perpetuity. All rights reserved. No reuse allowed without permission.

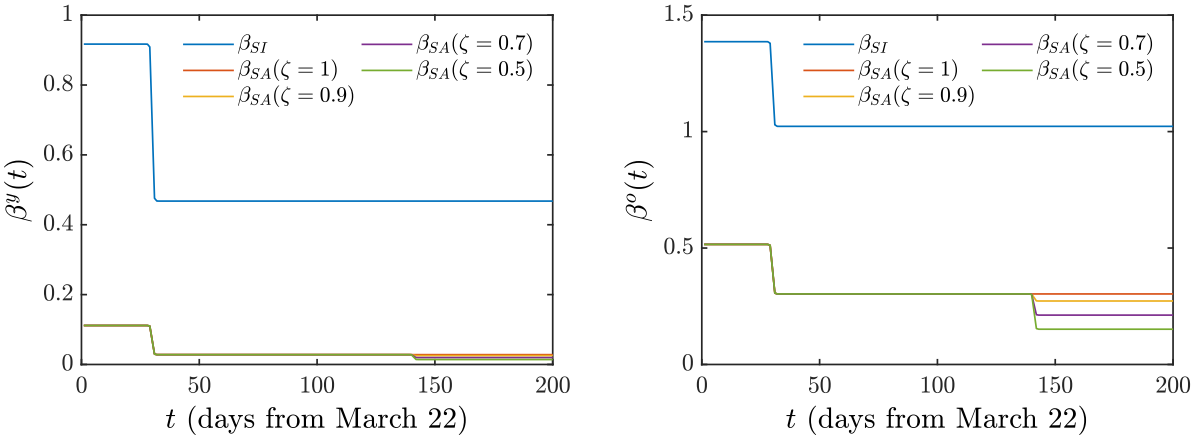

FIG. 9. Two-population model: Time dependence of β_{SI} and β_{SA} under the existing policy ($\zeta = 1$) and under the effect of additional (suggested) lockdown measures when applied to both populations (i.e. $\zeta^o = \zeta^y \equiv \zeta$).

TABLE V. Two-population model. Predictions for C and D at September 10 for parameters found by fitting the norm (8) when the measures are applied to both populations (i.e., $\zeta^o = \zeta^y \equiv \zeta$)

	$\zeta = 1$	$\zeta = 0.9$	$\zeta = 0.7$	$\zeta = 0.5$
C^y (total)	1636390	1617341	1582516	1551655
C^o (total)	182999	180063	174690	169916
$C^y + C^o$ (total)	1819389	1797404	1757206	1721571
C^y (from Aug. 10)	410217	391168	356344	325484
C^o (from Aug. 10)	45658	42722	37349	32576
$C^y + C^o$ (from Aug. 10)	455875	433890	393693	358060
D^y (total)	45538	45304	44865	44464
D^o (total)	33451	33213	32765	32351
$D^y + D^o$ (total)	78989	78516	77629	76815
D^y (from Aug. 10)	12495	12260	11821	11420
D^o (from Aug. 10)	9277	9038	8590	8177
$D^y + D^o$ (from Aug. 10)	21771	21298	20411	19597

(old) age group comes into contact with only old (young) infectious hosts. This form of community R_0 has been found in other contexts, such in HIV spread using a multi-group model [33]. Based on the parameter values found through our optimization procedure, it holds

$$R_0^{yy} = 1.6688, R_0^{oo} = 0.1897, R_0^{yo} = 4.5525, R_0^{oy} = 0.1614$$

and $R_0 = 2.0615$. We note that this is remarkably close to the R_0 of the one-population version of our model. The effective reproductive number at the beginning of social distancing measures ($t = t_q$) is $R_e = 1.5653$ with

$$R_e^{yy} = 1.2018, R_e^{oo} = 0.1582, R_e^{yo} = 3.7965, R_e^{oy} = 0.1340.$$

Upon imposition of the relevant measures, e.g., for $\zeta = 0.7$ or $\zeta = 0.5$, we have confirmed that both in the case of constraints only for the older population or in that of restrictive measures both the older and the younger population, it is true that $R_e < 1$.

IV. CONCLUSIONS AND FUTURE CHALLENGES

In the present work, we have proposed a model for the examination and fitting of the progression of the pandemic of COVID-19, with an aim towards applications to data given for different countries. The model has been developed to include susceptible

medRxiv preprint doi: https://doi.org/10.1101/2020.08.11.20172833; this version posted August 14, 2020. The copyright holder for this preprint (which was not certified by peer review) is the author/funder, who has granted medRxiv a license to display the preprint in perpetuity. All rights reserved. No reuse allowed without permission.

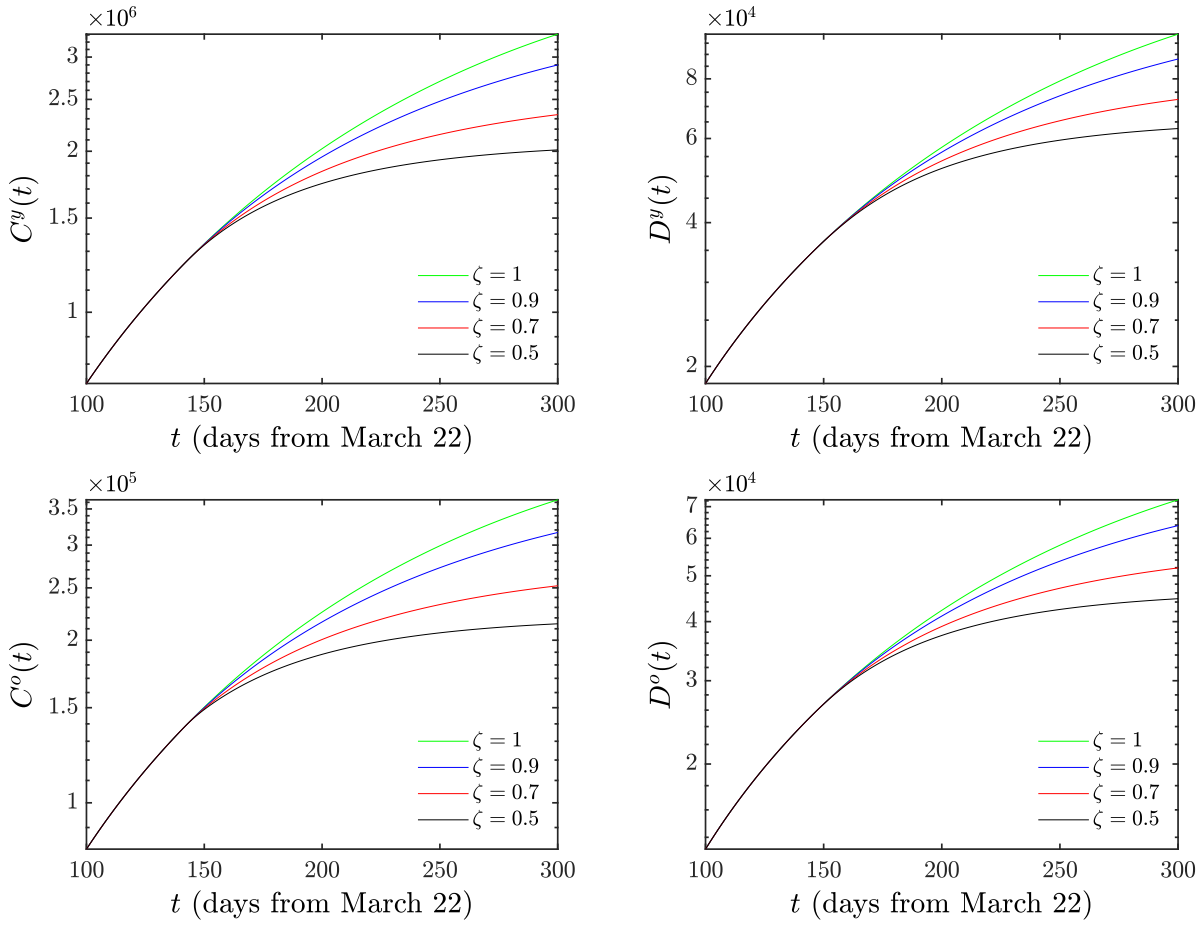

FIG. 10. Same as Fig. 8 but now with the restrictive measures applied from August 10 onward to both populations (i.e. $\zeta^o = \zeta^y \equiv \zeta$).

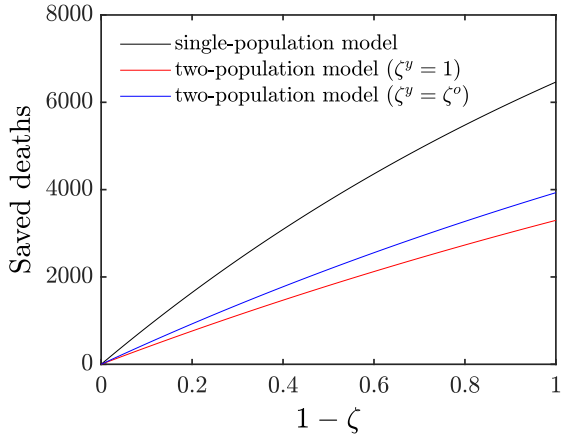

FIG. 11. Number of deaths that could be saved in the period Aug. 10 – Sep. 10 if the different measures discussed herein are applied.

individuals, turning to exposed upon an infectious interaction. Subsequently, these are split to presymptomatic or asymptomatic after a latent period. The asymptomatics can only recover, while the presymptomatics are led to an onset of symptoms. Subsequently, this can lead to either recovery or the need for hospitalization, and the latter again can either lead to recovery or to fatality. The model naturally involves assumptions that are not always met. E.g., in some cases people may die before getting a

medRxiv preprint doi: https://doi.org/10.1101/2020.08.11.20172833; this version posted August 14, 2020. The copyright holder for this preprint (which was not certified by peer review) is the author/funder, who has granted medRxiv a license to display the preprint in perpetuity. All rights reserved. No reuse allowed without permission.

chance to be hospitalized. In other settings where there is heavy testing involved, asymptomatics may be counted in the reported infections: while this is not an explicit assumption of the model, we did not count any fraction of asymptomatics in the cumulative infections when presenting the relevant comparison. Additionally, also, some of the hospitalized individuals may transmit the virus (e.g. to medical personnel) despite the much more substantial health and safety protocols applicable within hospitals. In any event, we consider these features to be the exception rather than the rule and hence have excluded them from our more mainstream considerations.

Within the realm of the model, we have exposed the meaning of the relevant parameters (e.g., transmission rates, latent and incubation times, fractions of asymptomatics vs. presymptomatics, of hospitalized vs. directly recovered, and of recovered vs. dying individuals at the hospital; also the time scales of the latter partitions were considered). I.e., we have attempted to assign an epidemiological meaning to our different parameters and to examine the associated results of the optimal fit of these parameters to the data from a specific time series to illustrate the "reasonable" nature of the findings. Notice that in addition to explaining the fitting process (to either deaths or deaths and cumulative infections), we have taken the approach of using a minimal number of assumptions to avoid constraining the system to the degree possible. We have also illustrated how the model can be partitioned to different age groups, based on the data that may be available for the country or region of interest. Here, we have opted to consider the simplest partition to 2-age models, yet while tedious, it is structurally straightforward (and of some interest in its own right) to generalize considerations to many age group models.

As our prototypical illustration of choice, we have used the case of data from Mexico which have been available through [28]. This is a case where a significant number of cases has arisen and the consideration of potential further lockdown measures is an important topic of ongoing debate. Indeed, our findings suggest that the present measures appear not to be sufficient to mitigate the catastrophic consequences of the pandemic, since the current value of the basic reproductive number of the epidemic is $R_0 > 1$ and hence the situation appears to need further mitigation measures and strategies to avoid significant loss of life. In that vein, we have discussed in the realm of the model what consequences different measures would have at the level of deaths and of cumulative infections. It was found, e.g., that a reduction of transmission rates by a factor of around $1/2$ via social distancing or related measures would lead to a nontrivial curbing of the rampant growth of both $C(t)$ and $D(t)$. The relevant reductions could of the order of 100000 in terms of infections and of more than 2000 in terms of deaths in the interval of the next 30 days alone. While our results are only suggestive (and relevant with the context of the model), we hope that they may be of some value towards policy considerations in the near future.

Naturally, there are numerous directions that are worthwhile to consider towards extensions of the present work. A natural feature of many of the models (e.g., associated with the US [15], but also elsewhere) is the incorporation of uncertainty. We are currently in the process of buidling into the formulation an uncertainty quantification framework on the basis of polynomial chaos considerations [34] and the use of suitable distributions for quantities such as the transmission rates. Constructing a robust such framework would be of considerable value to models such as the one proposed herein. In addition, as indicated in numerous cases, there are data broken down by age groups (e.g., not only for Mexico, but also for other countries such as Portugal [35], etc.). Clearly, a generalization of the model that considers the data by decade would offer a more complete and systematic picture of the impact of COVID-19 to different sub-populations and hence their potential risk. This would offer, in turn, a clearer picture of which age groups to attempt to protect and would be worthwhile (even if somewhat cumbersome). Lastly, as different countries are delving into a re-opening exercise, the formulation of a meta-population model with different hubs and a quantification of the transport coefficients between these [36] would be central towards going beyond the well-mixed assumption and factoring in a spatial structure and transportation features within the model. Such directions are currently under active investigation and will be reported in future work.

Appendix A: R_0 calculations

1. One-population model

We use the next generation matrix approach to find R_0 [31]. We define the relevant vectors:

$$\mathcal{F} = \begin{pmatrix} \beta_{SA}S(A+P) + \beta_{SI}SI \\ 0 \\ 0 \\ 0 \\ 0 \\ 0 \\ 0 \\ 0 \\ 0 \end{pmatrix}, \quad \mathcal{V} = \begin{pmatrix} \sigma_1 E \\ -(1-\phi)\sigma_1 E + \sigma_2 P \\ -\phi\sigma_1 E + M_{AR}A \\ -\sigma_2 P + MI \\ -\gamma MI + (1-\omega)\chi H + \omega\psi H \\ \beta_{SA}S(A+P) + \beta_{SI}SI + \mu S \\ -M_{AR}A \\ -(1-\gamma)MI - (1-\omega)\chi H \\ -\omega\psi H \end{pmatrix}$$

medRxiv preprint doi: https://doi.org/10.1101/2020.08.11.20172833; this version posted August 14, 2020. The copyright holder for this preprint (which was not certified by peer review) is the author/funder, who has granted medRxiv a license to display the preprint in perpetuity. All rights reserved. No reuse allowed without permission.

We then focus on the 5 infectious/infected compartments (E, P, A, I, H) and ignore the rest (S, A_R, R, D). We find the Jacobians of $\mathcal{F}, \mathcal{V}$ with respect to E, P, A, I, H in the order in which they appear. This will yield two 5×5 matrices:

$$F = \begin{pmatrix} 0 & \beta_{SA}S^* & \beta_{SA}S^* & \beta_{SI}S^* & 0 \\ 0 & 0 & 0 & 0 & 0 \\ 0 & 0 & 0 & 0 & 0 \\ 0 & 0 & 0 & 0 & 0 \\ 0 & 0 & 0 & 0 & 0 \end{pmatrix} \tag{A1}$$

$$V = \begin{pmatrix} \sigma_1 & 0 & 0 & 0 & 0 \\ -(1-\phi)\sigma_1 & \sigma_2 & 0 & 0 & 0 \\ -\phi\sigma_1 & 0 & M_{AR} & 0 & 0 \\ 0 & -\sigma_2 & 0 & M & 0 \\ 0 & 0 & 0 & -\gamma M & (1-\omega)\chi + \omega\psi \end{pmatrix} \tag{A2}$$

The basic reproductive number is the spectral radius of FV^{-1} which in our case is

$$R_0 = (1-\phi)\frac{\beta_{SA}S^*}{\sigma_2} + \phi\frac{\beta_{SA}S^*}{M_{AR}} + (1-\phi)\frac{\beta_{SI}S^*}{M}. \tag{A3}$$

The first term is due to the presymptomatic hosts P, the second due to the asymptomatic hosts A, and the last one due to the symptomatic infectious hosts I. In each term, the numerator yields the rate of new infections $\beta_{SA}S^*$, $\beta_{SI}S^*$ and this is then multiplied with the average duration of the stay in that infectious stage $\frac{1}{\sigma_2}$, $\frac{1}{M_AR}$, $\frac{1}{M}$. Each term is multiplied with the fraction of hosts in that stage/state ϕ for asymptomatics and $1-\phi$ for symptomatics.

2. Two-population model

Using again the next generation matrix approach results in the following two matrices:

$$F = \begin{pmatrix} 0 & \beta_{SA}^{yy}S^y & \beta_{SA}^{yy}S^y & \beta_{SI}^{yy}S^y & 0 & 0 & \beta_{SA}^{yo}S^y & \beta_{SA}^{yo}S^y & \beta_{SI}^{yo}S^y & 0 \\ 0 & 0 & 0 & 0 & 0 & 0 & 0 & 0 & 0 & 0 \\ 0 & 0 & 0 & 0 & 0 & 0 & 0 & 0 & 0 & 0 \\ 0 & 0 & 0 & 0 & 0 & 0 & 0 & 0 & 0 & 0 \\ 0 & 0 & 0 & 0 & 0 & 0 & 0 & 0 & 0 & 0 \\ 0 & \beta_{SA}^{oy}S^o & \beta_{SA}^{oy}S^o & \beta_{SI}^{oy}S^o & 0 & 0 & \beta_{SA}^{oo}S^o & \beta_{SA}^{oo}S^o & \beta_{SI}^{oo}S^o & 0 \\ 0 & 0 & 0 & 0 & 0 & 0 & 0 & 0 & 0 & 0 \\ 0 & 0 & 0 & 0 & 0 & 0 & 0 & 0 & 0 & 0 \\ 0 & 0 & 0 & 0 & 0 & 0 & 0 & 0 & 0 & 0 \\ 0 & 0 & 0 & 0 & 0 & 0 & 0 & 0 & 0 & 0 \end{pmatrix} \tag{A4}$$

$$V = \begin{pmatrix} \sigma_1 & 0 & 0 & 0 & 0 & 0 & 0 & 0 & 0 & 0 \\ -(1-\phi^y)\sigma_1 & \sigma_2 & 0 & 0 & 0 & 0 & 0 & 0 & 0 & 0 \\ -\phi^y\sigma_1 & 0 & M_{AR}^y & 0 & 0 & 0 & 0 & 0 & 0 & 0 \\ 0 & -\sigma_2 & 0 & M^y & 0 & 0 & 0 & 0 & 0 & 0 \\ 0 & 0 & 0 & -\gamma^y M^y & (1-\omega^y)\chi^y + \omega^y\psi^y & 0 & 0 & 0 & 0 & 0 \\ 0 & 0 & 0 & 0 & 0 & \sigma_1 & 0 & 0 & 0 & 0 \\ 0 & 0 & 0 & 0 & 0 & -(1-\phi^o)\sigma_1 & \sigma_2 & 0 & 0 & 0 \\ 0 & 0 & 0 & 0 & 0 & -\phi^o\sigma_1 & 0 & M_{AR}^o & 0 & 0 \\ 0 & 0 & 0 & 0 & 0 & 0 & -\sigma_2 & 0 & M^o & 0 \\ 0 & 0 & 0 & 0 & 0 & 0 & 0 & 0 & -\gamma^o M^o & (1-\omega^o)\chi^o + \omega^o\psi^o \end{pmatrix}. \tag{A5}$$

Since V is a block matrix it holds

$$V = \begin{pmatrix} A & 0 \\ 0 & D \end{pmatrix} \Rightarrow V^{-1} = \begin{pmatrix} A^{-1} & 0 \\ 0 & D^{-1} \end{pmatrix},$$

medRxiv preprint doi: https://doi.org/10.1101/2020.08.11.20172833; this version posted August 14, 2020. The copyright holder for this preprint (which was not certified by peer review) is the author/funder, who has granted medRxiv a license to display the preprint in perpetuity. All rights reserved. No reuse allowed without permission.

from which is readily follows that the spectral radius of FV^{-1} is given by

$$R_0 = \frac{R_0^{yy} + R_0^{oo}}{2} + \frac{\sqrt{(R_0^{yy} - R_0^{oo})^2 + 4R_0^{yo}R_0^{oy}}}{2}, \quad \text{where}$$

$$R_0^{yy} = (1-\phi^y)\frac{\beta_{SA}^{yy}S^y}{\sigma_2} + \phi^y\frac{\beta_{SA}^{yy}S^y}{M_{AR}^y} + (1-\phi^y)\frac{\beta_{SI}^{yy}S^y}{M^y}$$

$$R_0^{oo} = (1-\phi^o)\frac{\beta_{SA}^{oo}S^o}{\sigma_2} + \phi^o\frac{\beta_{SA}^{oo}S^o}{M_{AR}^o} + (1-\phi^o)\frac{\beta_{SI}^{oo}S^o}{M^o}$$

$$R_0^{yo} = (1-\phi^o)\frac{\beta_{SA}^{yo}S^y}{\sigma_2} + \phi^o\frac{\beta_{SA}^{yo}S^y}{M_{AR}^o} + (1-\phi^o)\frac{\beta_{SI}^{yo}S^y}{M^o}$$

$$R_0^{oy} = (1-\phi^y)\frac{\beta_{SA}^{oy}S^o}{\sigma_2} + \phi^y\frac{\beta_{SA}^{oy}S^o}{M_{AR}^y} + (1-\phi^y)\frac{\beta_{SI}^{oy}S^o}{M^y}.$$

R_0^{yy} and R_0^{oo} are the basic reproductive numbers in the young and old age groups, respectively, if they were completely isolated of each other. R_0^{yo} is the basic reproductive number if susceptible young hosts come into contact with only old infectious hosts, and R_0^{oy} is the basic reproductive number if old hosts come into contact with only young infectious hosts.

Acknowledgments This material is based upon work supported by the US National Science Foundation under Grants No. DMS-1815764 (ZR), PHY-1602994, and DMS-1809074 (PGK). PGK also acknowledges support from the Leverhulme Trust via a Visiting Fellowship and thanks the Mathematical Institute of the University of Oxford for its hospitality during this work.

Disclaimer The views expressed in this manuscript are purely those of the authors and may not, under any circumstances, be regarded as an official position of the European Commission.

---

[1] https://www.who.int/emergencies/diseases/novel-coronavirus-2019
[2] W.O. Kermack, A.G. McKendrick, Proc. Roy. Soc. A **115**, 700 (1927).
[3] H. Hethcote, SIAM Rev. **42**, 599 (2000).
[4] N.T.J. Bailey, *The mathematical theory of infectious diseases and its applications*, Griffin (London, 1975).
[5] R.M. May, R.M Anderson, *Infectious diseases of humans: dynamics and control*, Oxford University Press (Oxford, 1991).
[6] F. Brauer, C. Castillo-Chávez, *Mathematical Models in Population Biology and Epidemiology*, Springer-Verlag (New York, 2001).
[7] Z.-Q. Xia, J. Zhang, Y.-K. Xue, G.-Q. Sun, Z. Jin, PLoS One **10**, e0144778 (2015).
[8] X. Hao, *et al.*, Nature, https://doi.org/10.1038/s41586-020-2554-8 (2020).
[9] M. M. Arons *et al.*, Presymptomatic SARS-CoV-2 infections and transmission in a skilled nursing facility, NEJM, DOI: 10.1056/NEJMoa2008457.
[10] M. Peirlinck, K. Linka, F.S. Costabal, J. Bhattacharya, E. Bendavid, J.P.A. Ioannidis, E. Kuhl https://doi.org/10.1101/2020.05.23.20111419
[11] E. J. Emanuel *et al.*, N Engl J Med **382**, 2049-2055 (2020).
[12] J. B. Dowd *et al.*, PNAS **117**, 9696-9698 (2020).
[13] Z. Zheng *et al.*, J. of Infection **81**, e16-e25 (2020).
[14] M.R. Nepomuceno *et al.*, PNAS **117**, 13881-13883 (2020).
[15] For instance in the models reported in: https://www.cdc.gov/coronavirus/2019-ncov/covid-data/forecasting-us.html for modeling the US, only one (Northeastern) appears to be focusing on age-structured modeling [see, e.g., https://covid19.gleamproject.org/ and references therein].
[16] J. E. Ludvigsson, Acta Paediatrica **109** 1088–1095 (2020).
[17] K. Xu *et al.*, Clinical Infectious Diseases **71**, 799-806 (2020).
[18] J. Mossong *et al.*, PLoS Med **5**, 374 (2008).
[19] O. Torrealba-Rodriguez, R. A. Conde-Guttiérrez, A. L. Hernández-Javier, Chaos, Solitons and Fractals **138**, 109946 (2020).
[20] M. Anzarut *et al.*, https://arxiv.org/abs/2007.09117
[21] U. Avila-Ponce de León, A. G. C. Pérez, E. Avila-Vales, https://arxiv.org/abs/2004.08288
[22] J. P. Gutierrez and S. M. Bertozzi, https://www.medrxiv.org/content/10.1101/2020.05.27.20115204v2
[23] P.G. Kevrekidis, J. Cuevas-Maraver, Y. Drossinos, Z. Rapti, G.A. Kevrekidis, arXiv:2005.04527.
[24] See, e.g., https://elifesciences.org/articles/57309
[25] N.I. Stilianakis and Y. Drossinos, J. R. Soc. Interface **7**, 1355 (2010).
[26] Y. Drossinos and N.I. Stilianakis, Aerosol Sci. Technol. **54**, 639 (2020).
[27] D.K. Milton, M. Patricia Fabian, B.J. Cowling, M.L. Grantham, J.J. McDevitt, PLoS Pathog. **9**, e1003205 (2013).
[28] https://www.gob.mx/salud/documentos/datos-abiertos
[29] A.A. King, M. Domenech de Cellés, F.M.G. Magpantay, P. Rohani, Proc. Roy. Soc. B **282**, 20150347 (2015).
[30] M.C. Eisenberg, S.L. Robertson, J.H. Tien, J. Theor. Biol. **324**, 84 (2013).

medRxiv preprint doi: https://doi.org/10.1101/2020.08.11.20172833; this version posted August 14, 2020. The copyright holder for this preprint (which was not certified by peer review) is the author/funder, who has granted medRxiv a license to display the preprint in perpetuity. All rights reserved. No reuse allowed without permission.

[31] O. Diekmann, J. A. P. Heesterbeek, and J. A. J. Metz, Journal of Mathematical Biology **28**, 365–382 (1990).
[32] A.S. Fokas, J. Cuevas-Maraver, P.G. Kevrekidis, https://doi.org/10.1101/2020.05.08.20095380.
[33] J. M. Hyman and J. Li, SIAM J Appl. Math. **57** 1082-1094 (1997).
[34] D. Xiu and G. Em. Karniadakis, SIAM J. Sci. Comput. **24**, 619 (2002).
[35] https://github.com/dssg-pt/covid19pt-data
[36] R. Li et al., Science **368**, 489 (2020).